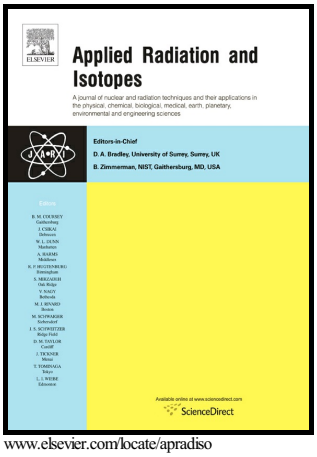

www.elsevier.com/locate/apradiso

Extending neutron autoradiography technique for boron concentration measurements in hard tissues

Lucas Provenzano, María Silvina Olivera, Gisela Saint Martin, Luis Miguel Rodríguez, Daniel Fregenal, Silvia I. Thorp, Emiliano C.C. Pozzi, Paula Curotto, Ian Postuma, Saverio Altieri, Sara J. González, Silva Bortolussi, Agustina Portu

PII: S0969-8043(17)30921-1
DOI: https://doi.org/10.1016/j.apradiso.2018.03.011
Reference: ARI8294

To appear in: *Applied Radiation and Isotopes*

Received date: 3 August 2017
Revised date: 23 January 2018
Accepted date: 10 March 2018

Cite this article as: Lucas Provenzano, María Silvina Olivera, Gisela Saint Martin, Luis Miguel Rodríguez, Daniel Fregenal, Silvia I. Thorp, Emiliano C.C. Pozzi, Paula Curotto, Ian Postuma, Saverio Altieri, Sara J. González, Silva Bortolussi and Agustina Portu, Extending neutron autoradiography technique for boron concentration measurements in hard tissues, *Applied Radiation and Isotopes,* https://doi.org/10.1016/j.apradiso.2018.03.011

Extending neutron autoradiography technique for boron concentration measurements in hard tissues.

Lucas Provenzano[a,b], María Silvina Olivera[a], Gisela Saint Martin[a], Luis Miguel Rodríguez[a,b], Daniel Fregenal[a,b], Silvia I. Thorp[a], Emiliano C.C.Pozzi[a], Paula Curotto[a], Ian Postuma[c], Saverio Altieri[c,d], Sara J. González[a,b], Silva Bortolussi[c,d] and Agustina Portu[a,b]

[a] Comisión Nacional de Energía Atómica (CNEA), Av. Del Libertador 8250, C1429BNP, CABA, Argentina.

[b] Consejo Nacional de Investigaciones Científicas y Técnicas (CONICET), Godoy Cruz 2290, C1425FQB, CABA, Argentina.

[c] Istituto Nazionale di Fisica Nucleare (INFN), Unit of Pavia, via A. Bassi 6, 27100, Pavia, Italy.

[d] Departament of Physics, University of Pavia, via A. Bassi 6, 27100 Pavia, Italy.

Corresponding author:

Agustina Mariana Portu. Department of Radiobiology, National Atomic Energy Commission (CNEA), Av. General Paz 1499, B1650KNA, San Martin, Buenos Aires, Argentina. Tel.:54-11-6772-7933/7150. E-mail: agustina.portu@gmail.com - portu@cnea.gov.ar.

Other authors e-mail:

provenza@tandar.cnea.gov.ar
olivera@cnea.gov.ar
gisaint@cnea.gov.ar
lmr@cab.cnea.gov.ar
fregenal@cab.cnea.gov.ar
thorp@cae.cnea.gov.ar
epozzi@cnea.gov.ar
curotto@cae.cnea.gov.ar
saverio.altieri@pv.infn.it
ian.postuma@pv.infn.it
srgonzal@cnea.gov.ar
silva.bortolussi@pv.infn.it

Abstract

The neutron autoradiography technique using polycarbonate nuclear track detectors (NTD) has been extended to quantify the boron concentration in hard tissues, an application of special interest in Boron Neutron Capture Therapy (BNCT).

Chemical and mechanical processing methods to prepare thin tissue sections as required by this technique have been explored. Four different decalcification methods governed by slow and fast kinetics were tested in boron-loaded bones. Due to the significant loss of the boron content, this technique was discarded. On the contrary, mechanical manipulation to obtain bone powder and tissue sections of tens of microns thick proved reproducible and suitable, ensuring a proper conservation of the boron content in the samples.

A calibration curve that relates the ^{10}B concentration of a bone sample and the track density in a Lexan NTD is presented. Bone powder embedded in boric acid solution with known boron concentrations between 0 and 100 ppm was used as a standard material. The samples, contained in slim Lexan cases, were exposed to a neutron fluence of 10^{12} cm^{-2} at the thermal column central facility of the RA-3 reactor (Argentina). The revealed tracks in the NTD were counted with an image processing software. The effect of track overlapping was studied and corresponding corrections were implemented in the presented calibration curve.

Stochastic simulations of the track densities produced by the products of the ^{10}B thermal neutron capture reaction for different boron concentrations in bone were performed and compared with the experimental results. The remarkable agreement between the two curves suggested the suitability of the obtained experimental calibration curve.

This neutron autoradiography technique was finally applied to determine the boron concentration in pulverized and compact bone samples coming from a sheep experimental model. The obtained results for both type of samples agreed with boron measurements carried out by ICP-OES within experimental uncertainties. The fact that the histological structure of bone sections remains preserved allows for future boron microdistribution analysis.

Highlights

- The neutron autoradiography technique was extended to measure boron in bone.

- A reference system was developed for boron concentration measurements in bone.

- Stochastic simulations of tracks generation were compared with measurements.

- The developed system was validated by ICP-OES measurements of sheep bone.

Keywords

BNCT, bone, neutron autoradiography

1. Introduction

Nuclear track detectors (NTD) are widely used for heavy ion detection, the mapping of elements being one of its outstanding applications (Durrani and Bull 1987).. As the particle impacts the detector, it damages the region along its trajectory. The so called “latent tracks” have a radial dimension of a few nanometers, but they can be enlarged or “revealed” by a chemical etching, in order to be visible to electronic or optical microscopy. The etching reagents preferentially attack the damaged regions rather than the undamaged ones (Fleischer et al. 1975).

The track analysis technique has been widely used for several applications, ranging from radon measurements, personal dosimetry, fossil dating, among others [3]. In particular, if the NTD is put in contact with a sample containing the isotope ^{10}B and the whole assembly is exposed to a thermal neutron flux ($E_n \leq 0.5$ eV), the boron neutron capture reaction (BNC) takes place:$^{10}B(n,alpha)^{7}Li$. The alpha and ^{7}Li high linear energy transfer particles are emitted oppositely (180°) and lose their energy in few micrometers. As each nuclear track corresponds to a single thermal neutron capture reaction by ^{10}B, boron concentration in the sample can be determined by counting the etched pits. Besides, tracks location on the NTD reflect boron atoms positions in the sample (mapping of boron distribution). This is the basis of the application of the neutron autoradiography technique to study boron macro and microdistribution in samples coming from Boron Neutron Capture Therapy (BNCT) protocols, extensively developed in Altieri et al. (2008) and Portu et al. (2015).

BNCT is a combined cancer treatment consisting in the administration of a ^{10}B-enriched compound to the patient, and the subsequent irradiation with thermal neutrons of the zone to be treated. The products of the BNC reaction deposit their energy in tissue over distances comparable to the size of a mammalian cell. Thus, if the boron compound is selectively targeted to the neoplastic cells, the surrounding normal tissue is ideally preserved (Barth et al. 2012). BNCT involves biochemical rather than geometrical targeting, thus knowledge of the macro and

microdistribution of boron in tissues is pivotal for the dosimetry and treatment planning in this therapy. Since its first proposal (Locher 1936), BNCT has been applied in several countries, mainly for the treatment of primary and recurrent glioblastoma, head and neck tumors and cutaneous melanoma (e.g., Barth et al. 2012, Kato et al. 2004, Kankaanranta et al. 2012, Wang et al. 2011, González et al., 2004). Over the last years, other tumor targets have been explored, as liver metastases (Zonta et al. 2006, Yanagie et al. 2014), lung tumors (Suzuki et al. 2006) and osteosarcoma (Kato et al. 2004, Futamura et al. 2014). Particularly, osteosarcoma is the most common primary malignant bone tumor (Bielack et al. 2009). As it could be a possible target for BNCT, several aspects of this malignancy, such as boron uptake either in soft and hard dose-limiting normal tissues and tumors, should be addressed. Moreover, when treating head and neck or brain tumors with BNCT, neighbor bone could absorb a dose higher than the tolerance level, thus resulting in potentially dangerous side effects. For this reason, a reliable method to determine boron concentration in bone is required for a safe and effective treatment plan assessment.

Recently, in vitro and in vivo osteosarcoma models have been used to assess boron uptake on the UMR-106 osteosarcoma cell line (Ferrari et al. 2009, Postuma et al. 2016), and to determine the ^{10}B distribution in normal and tumor tissue sections (Bortolussi et al. 2017). Essentially, two nuclear techniques were employed for this purpose: alpha spectrometry (Bortolussi and Altieri 2013) and neutron autoradiography (Portu et al. 2015). However, since both techniques had been developed and optimized for liquid and/or soft tissue samples, the quantification of the boron concentration in hard tissues such as normal bone presented some limitations. The structure of bone tissue and of certain osteosarcoma tumors is significantly different from that of soft tissue. The main reason is the classification of the extracellular components that confers it hardness. Given that the energy deposition of the alpha and Li ions along their paths in tissues strongly depends on the elemental composition and density of the material, the application of the mentioned nuclear techniques for boron analysis in hard tissues requires further development.

This work deals with the extension of the neutron autoradiography technique for boron measurements in hard tissues, particularly in bone. A calibration curve that relates boron concentration in the sample with track density on the nuclear track detector is here presented. The construction of this curve required generating samples with known amounts of boron. As described in (Saint Martin et al. 2011), these standards must meet two requirements: to present a structure similar to the sample to be measured and to ensure a uniform distribution of generated tracks on

the detector. Thus, a detailed report on the development of suitable standards is also provided.

An interesting feature of the neutron autoradiography technique is the possibility of studying how the boron is distributed in the histological structures of the sample, provided that thin tissue sections can be obtained. Within this context, two strategies for constructing thin bone sections are discussed: a process of chemical decalcification and the polishing of samples up to micrometer scale.

Finally, the neutron autoradiography technique, based on the results reported here, is applied to determine the unknown boron concentration of bone samples coming from sheep. Comparisons with an independent boron measurement technique are discussed.

2. Material and methods

2.1 Preliminary studies

As mentioned above, the calcification of extracellular components confers hardness to tissues such as bone. Due to this property, a decalcification process must precede sectioning. Applying different chemical processes that decrease the amount of calcium, it is possible to adequate the consistency of hard tissue samples to be sliced by a conventional cryostat. In this way, samples could be analyzed by neutron autoradiography using methodologies previously developed for soft tissue (Postuma et al. 2016, Portu et al. 2011).

Femur samples from sheep subjected to a boronophenylalanine (BPA) biodistribution protocol (BPA dose of 350 mg/kg i.v. infused over 45 minutes) (Farias et al. 2015) were obtained to study different decalcifying methods (Provenzano et al. 2015). Four protocols were tested immersing the samples in: (a) ethylenediaminetetraacetic acid (EDTANa 0.5M) and sodium hydroxide (NaOH pH ~ 8.5), (b) hydrochloric acid (1.85%) and formic acid (4.75%), (c) nitric acid (6.5%) and (d) nitric acid (7.5%) and formaldehyde (5%). For the first protocol, characterized by a slow decalcifying process, three samples were immersed in EDTA disodium for one, two and three weeks, respectively. For the other three protocols, characterized by fast kinetics, one sample was immersed for 24 hours. Non-treated bone samples were used as control.

During the experiment, the consistency of the samples was measured. Portions of both decalcified and control samples were digested in 30% nitric acid solution to measure the boron and calcium concentration by Inductive Coupled Plasma – Optic Emission Spectroscopy (ICP-OES). An experimental uncertainty of ±8% was

established for this measurement methodology. The supernatant was also measured by High Performance Liquid Chromatography (HPLC) in order to verify the presence of boron in the solution.

The optimal time of decalcifying process was assessed for each of the tested protocols. The best immersion time suitable for cryostat processing was obtained after 3 weeks for protocol (a), 24 hours for protocols (b) and (d) and 42 hours for protocol (c). Under these conditions, however, significant boron loss was observed. HPLC and ICP-OES measurements confirmed that the sample lost about 97% of their boron concentration along with calcium (Provenzano et al. 2014). These findings precluded the use of decalcified bone sections for boron measurement purpose.

2.2 Calibration Samples

Bone powder was then studied as a possible replacement of thin sections for neutron autoradiography. The powder was generated by milling non-treated sheep femur using a lathe with a sterilized diamond saw to prevent contamination. In this way, the loss of any bone component was avoided and the original elemental composition was preserved. The preservation of boron content during the milling process was tested by ICP-OES measurements.

Reference standards were prepared by soaking the sheep femur powder in boric acid solutions ranging from 0 to 100 ppm. Assuming total water evaporation of the solution and no boron loss, the final boron concentration of the standard ($\mathrm{B_{std}}$) in parts per million was determined by:

$$\mathrm{B_{std}} = \frac{\mathrm{m_{ba} * B_{ba}}}{\mathrm{m_{bp.}}} + \overline{\mathrm{B}}_{\mathrm{bp}}^{\mathrm{nat}}, \qquad (1)$$

where $\mathrm{m_{ba}}$ is the mass of the boric acid in grams, $\mathrm{B_{ba}}$ is the ^{10}B concentration of boric acid in parts per million, $\mathrm{m_{bp}}$ is the mass of bone powder in grams, and $\overline{\mathrm{B}}_{\mathrm{bp}}^{\mathrm{nat}}$ is the mean concentration of natural ^{10}B in bone powder. The boron concentration values obtained in the powder samples (from here on “nominal concentration values”) were later confirmed by ICP-OES measurements.

The NTD selected for this study was polycarbonate (Lexan^{TM}). After drying in a vacuum bell, the boronated powder was placed into Lexan cases of 0.01 cm^3 fabricated for this purpose as reported in (Portu et al. 2011). The assemblies were exposed to a neutron fluence of 10^{12} cm^{-2} at the thermal column central facility (FCCT) of the RA-3 reactor (Argentina).

An etching process with PEW solution (30 g KOH+80 g ethyl alcohol+90 g distilled water) at 70ºC for 2 min was then performed to reveal the latent tracks produced by the particles resulting from the boron neutron capture reaction.

2.3 Image processing

Several microscopic images covering the surface of the revealed Lexan foils were taken with a Carl Zeiss MPM 800 microscope, at an original magnification of 40x. The number of tracks per image was determined using image processing software (Image Pro Premier^{TM} 2009). Due to scratches produced by the powder movement inside the Lexan cases, it was necessary to set up two digital image filters before counting. A first grey scale threshold filter was applied to avoid the inhomogeneous field of the microscope light over the sample background. A second filter was applied by rejecting tracks smaller than a fixed size in order to remove artefacts that do not correspond to real tracks.

For certain track densities, overlapping of events can significantly affect the assessment of the boron concentration in the sample. To take this effect into account, several images were computationally generated for different track densities. To this end, experimental track area distribution had to be determined to be used as an input. Tracks were counted with the same image processing software as the experimental ones. The ratio between the number of generated tracks and the number of counted tracks was applied as a correction factor to the software-assisted counting.

2.4 Simulations

Following the work by Saint Martin et al. (2011) , a stochastic simulation of tracks density produced by the neutron capture of boron in bone was performed and compared with the experimental results. The Monte Carlo model proposed by these authors is capable to estimate the number of tracks produced in a given NTD material by a sample containing ^{10}B atoms. The code requires as input information the stopping power of alpha particles and lithium in the material of the sample of interest. In this work, the stopping power for sheep femur was determined with SRIM software (Ziegler et al. 1985) using the elemental composition measured with PIXE technique (Johnson et al. 1970).

The PIXE measurements were carried out in a NEC 5SDH, 1.7 MV Tandem Accelerator at Centro Atómico Bariloche (Argentina). Thin samples of sheep femur (~100 µm) were disposed in the vacuum chamber of the facility and irradiated with

protons of 2 MeV. The Sirius SD detector was placed 33º apart from the beam line to collect the scattered X rays. The elemental composition of the sample was determined from the spectrum by reverse engineering using GUPIX [29]. As this technique cannot measure elements lighter than carbon, the hydrogen proportion was added according to the mean relative value reported in the bibliography for bone composition (ICRU Report No. 46 1992).

The Monte Carlo simulations were performed for the same boron concentration of the experimental standards and estimated values were corrected using the adjusting factor reported in Saint Martin et al. (2011) that accounts for differences between the experimental data and simulations.

2.5 Measurements in samples with unknown boron concentration

Sheep bone samples from the same series as those used for the decalcifying process were measured by neutron autoradiography to determine boron concentration: a non-boron loaded sample (femur: A) and boron-loaded samples coming from BPA biodistribution studies in sheep (femur: B,C,D, rib: E). Boron concentration values were determined preparing bone powder and using the calibration curve assessed in this work.

An alternative preparation process usually applied to study fossil bones for dating studies using track analysis (e.g. Jolivet et al. 2008) was also explored with the aim to preserve the histological structure of the tissue for potential analysis of boron microdistribution in bone. For this purpose, thin sections obtained by polishing the samples up to micrometer scale (100 µm) were also analyzed.

Finally, results obtained with neutron autoradiography were compared with ICP-OES measurements.

3. Results and Discussion

The generation of bone powder proved to be reproducible and affordable in a reasonable time, using the tools available at the laboratory. The efficiency of the grinding process using a diamond saw is low because a certain loss of material cannot be avoided. Nevertheless, the protocol allowed the production of enough powder for all the validation measurements as well as for the calibration curve determination.

The fact that the milling process does not affect the original boron concentration was checked by ICP-OES measurements of compact and powder bone. The results of the comparison are shown in Table I. As can be seen observed, values agree within their associated uncertainties except for sample D for which the estimated boron concentration of bone powder is slightly higher than that of the compact bone. However, it will be shown below that these values assessed by neutron autoradiography agree within uncertainties. For this reason, bone powder can be used for boron measurements.

Table I Comparison of ICP-OES measurements of boron concentration (ppm) in compact bone and in powder.

Sheep femur	Compact samples	Powder
A	0.44 ± 0.04	0.42 ± 0.03
B	1.5 ± 0.1	1.6 ± 0.1
C	3.3 ± 0.3	3.6 ± 0.3
D	4.3 ± 0.3	5.5 ± 0.5

The next phase to create bone standards (with known boron concentration) was supplying boric acid to samples of non-treated bone powder. Samples with boric acid were put in a vacuum bell to dry; the optimal drying time for re-milling was experimentally determined to be 24 hours.

In order to characterize the described method, the created standard samples were measured by ICP-OES. Additional measurements of untreated compact bones confirm the presence of a mean concentration of 0.5 ppm of natural ^{10}B that was used to correct the calculation of nominal concentration. Figure 1 shows that a linear correspondence was obtained between the nominal concentration of the reference samples and the measured concentration. Measurements agree with nominal values within uncertainties in the whole range of concentrations, thus allowing the latter to be assumed as the concentration of the reference standard.

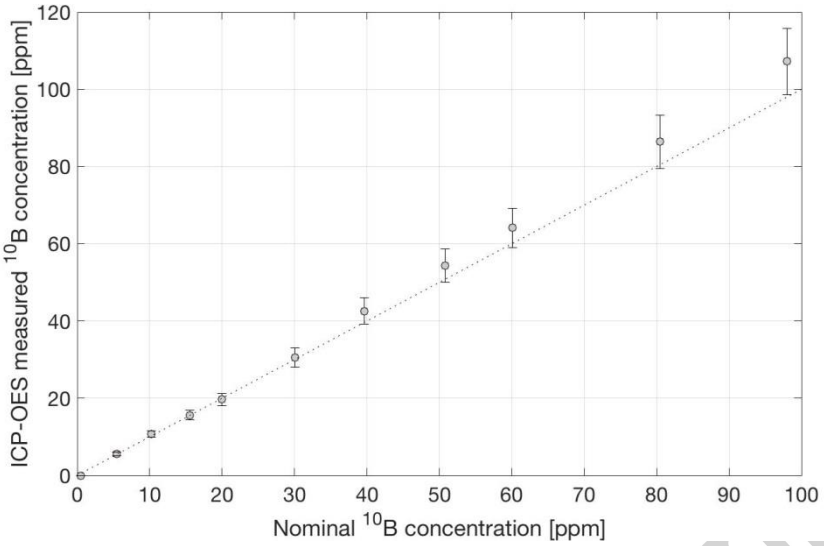

Figure 1: Measured ^{10}B concentration in the standard samples by ICP-OES as a function of the corresponding nominal values. The dashed curve represents the $\mathbf{y} = \mathbf{x}$ straight line.

The Lexan cases containing standards were then irradiated and the analysis of tracks density was carried out. Pits were clearly observed with an optical microscope and they were counted as a whole, as reported in Portu et al. 2011. A microscopic inspection along the central axis of a representative image suggested that bone powder samples produce nearly uniform track distributions adequate for the proposed technique. These findings showed the suitability of boronated bone powder as a reference system for the determination of boron concentration values in bone samples by neutron autoradiography.

This first overview also evidenced the mechanical sensibility of Lexan. Figure 2a shows that some scratches were detected in the autoradiography image, possibly generated by the relative movement of bone powder inside the polycarbonate cases. This fact, that usually does not occur with soft tissue sections deposited on Lexan, required the set-up of a filtering process to eliminate the background. Figure 2 depicts an example of the image filtering process implemented in this work: the final image (Fig. 2b) allows an automatic counting that is not possible in the original image (Fig. 2a).

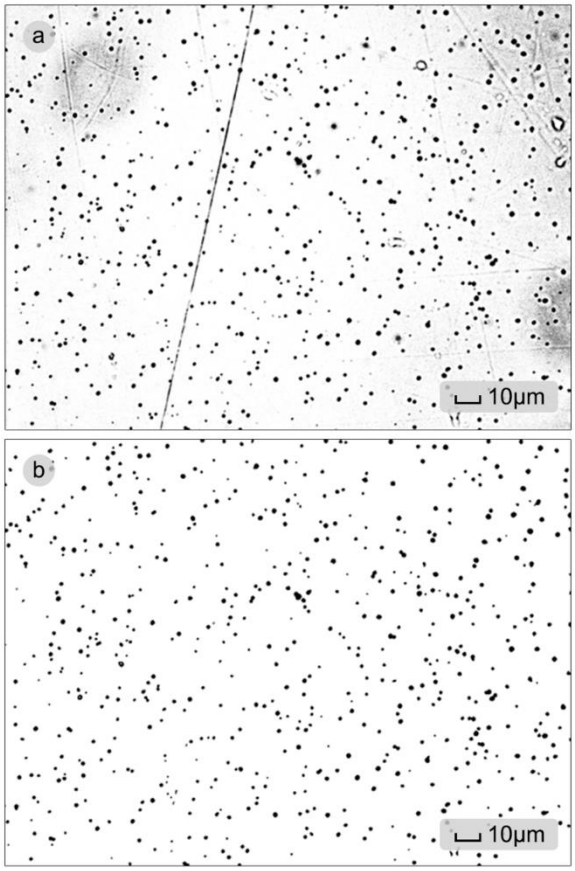

Figure 2: a) Original microphotograph of tracks b) Resulting filtered image.

The calibration curve was constructed by measuring the nuclear track density over 30 images per standard sample. The impact of tracks overlapping on the total number of counts was also studied and a correction factor was determined. As Figure 3 shows, the computationally-generated image looks very similar to the corresponding to reference samples with the same number of detected tracks. The ratio between the generated and detected tracks density in the artificial images as a function of the detected track density is shown in Figure 4, along with the fitted model used to correct the effect of tracks overlapping in all the samples.

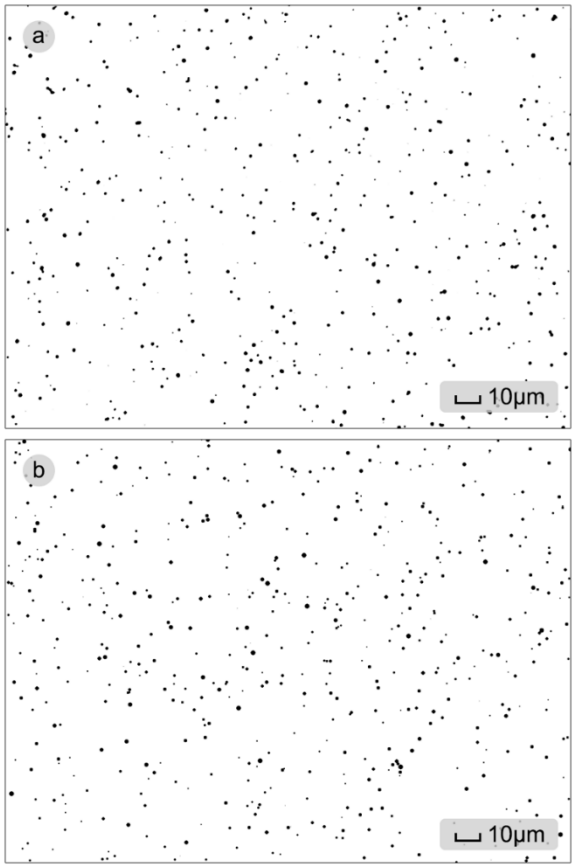

Figure 3: a) Image of 550 tracks digitally counted from a 60ppm standard sample. b) Image of 550 tracks generated digitally.

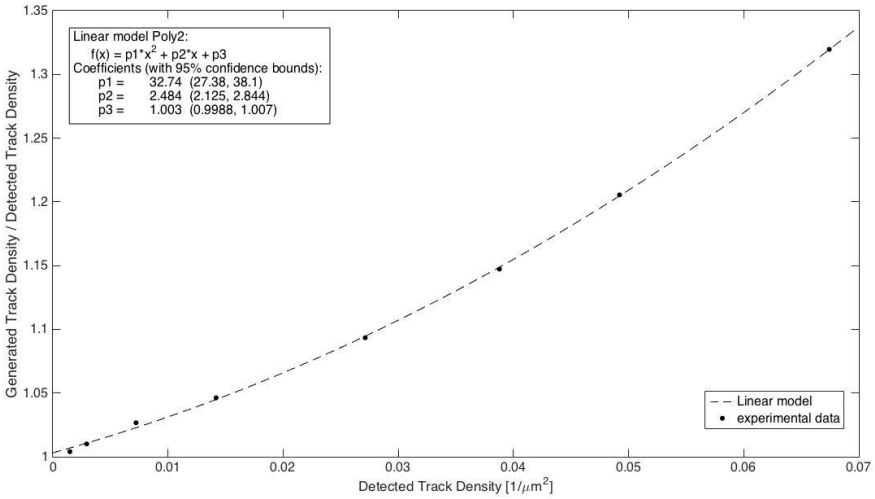

Figure 4: Quadratic behavior of the ratio between the generated track density and the detected track density.

Figure 5 depicts the experimental calibration curve for boron concentration determinations in bone by neutron autoradiography. As expected (after considering the overlapping effect), a linear relationship between the number of tracks per surface unit area and the ^{10}B concentration in reference samples for a thermal neutron fluence of 10^{12} cm^{-2} was found.

It is important to remark that the obtained calibration curve provides information of boron concentration for tracks density between 0 and 0.045 tracks/μm^2. According to Figure 4, the overlapping correction reaches values between 15% and 20% for the highest densities. However, this result is associated to the neutron fluence chosen for this particular study. As it is proportional to track density, the correction could be of greater relevance for higher neutron fluences commonly used in neutron autoradiography techniques (Portu et al. 2011).

The estimated calibration curve based on the stochastic calculations that took into account the measured bone elemental composition by PIXE is also shown in Figure 5. The two curves show a remarkable agreement, thus reinforcing the suitability of the obtained experimental calibration.

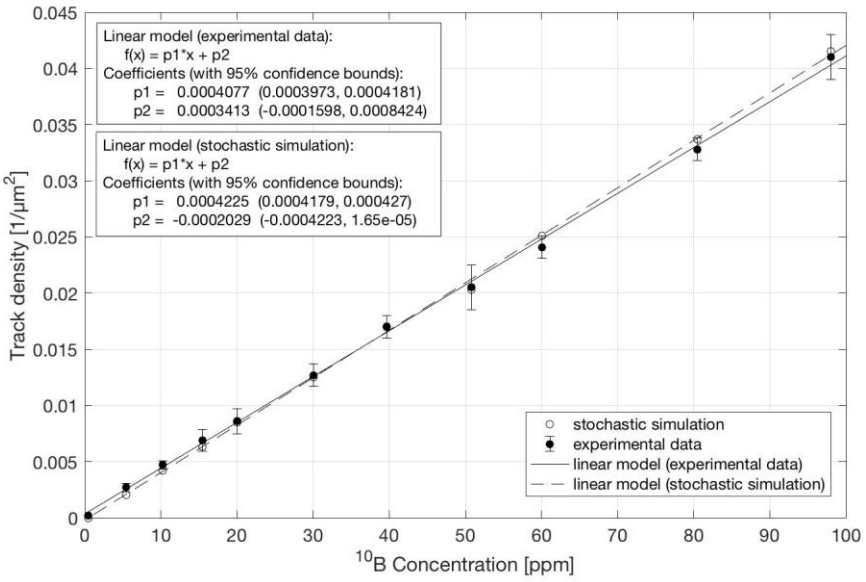

Figure 5: Calibration curve for autoradiography in bones irradiated with a neutron fluence of 10^{12} cm^{-2}.

The method of neutron autoradiography based on the calibration curve obtained as described above was applied to assess boron concentration values in bone samples taken from different boron biodistribution studies. Measurements by

neutron autoradiography were carried out both in powder and in thin sections, when possible.

The comparison between the neutron autoradiography values and the ICP-OES results are shown in Table II. ICP-OES values correspond to the average results reported in Table I assuming equality between compact bone and powder. Error bars corresponding to autoradiography results were obtained from the least square approximation equation (Skoog and Leary 1996). It can be seen that this technique allows the determination of boron concentration values above 2 ppm, which is comparable to the resolution for soft tissue (Portu et al. 2015a).

Table II Boron concentration (ppm) of sheep bone samples measured with neutron autoradiography. ICP-OES average values are also shown for comparison.

Bone sample	Compact	Powder	ICP-OES
A	-	0.4 ± 2.1	0.43 ± 0.04
B	1.3± 2.1	1.0 ± 2.0	1.6 ± 0.2
C	3.6 ± 1.9	3.6 ± 1.9	3.5 ± 0.5
D	4.9 ± 1.9	5.2 ± 1.9	4.9 ± 0.4
E	10.9 ± 1.5	-	8.9 ± 0.7

The results of neutron autoradiography confirm that boron concentration values of powder and compact samples agree within uncertainties. These uncertainties were calculated as the quadratic sum of the standard deviation in the tracks counting, and the nominal error of the interpolation process. They are around 2 ppm, as those previously calculated for individual samples of soft tissue (e.g. Portu et al., 2015a, Portu et al., 2015b). This correspondence is of great relevance because it allows the calibration curve constructed from powder samples to be used for the analysis of thin sections. The histological structure preservation of the bone sections is essential for future boron microdistribution analysis, which is the main advantage of neutron autoradiography over other boron determination techniques.

In addition, neutron autoradiography results are in agreement with ICP-OES values, thus demonstrating that the calibration set-up is suitable for boron content assessment in bone.

4. Conclusions

In this work, a methodology for the processing and autoradiographic analysis of bone samples was established. A calibration curve in the range of boron concentration values of interest in BNCT was constructed and validated both by stochastic simulations and by an independent reference method (ICP-OES).

Samples of unknown boron concentration were measured using this technique and the results were also confirmed by ICP-OES. Finally, the equivalence between both compact and powder bone neutron autoradiography results and boron measurements by ICP-OES paves the way for the analysis of boron microdistribution of normal bone and samples coming from osteosarcoma models. This information is of great relevance for evaluating BNCT feasibility studies.

Acknowledgements

This work was partially funded by the AGENCIA NACIONAL DE PROMOCIÓN CIENTÍFICA Y TECNOLÓGICA of Argentina through a PICT grant Nº 2013-1777, and by the CONSEJO NACIONAL DE PROMOCIÓN CIENTÍFICA Y TÉCNICA (CONICET) through a PIP grant Nº112 201301 00458 CO.

References

Altieri, S., Bortolussi, S., Bruschi, P., Chiari, P., Fossati, F., Stella, S., Prati, U., Roveda, L., Zonta, A., Zonta, C., Ferrari, C., Clerici, A., Nano, A., Pinelli, T., 2008. Neutron autoradiography imaging of selective boron uptake in human metastatic tumours, Appl. Rad. Isot. 66:1850-5.

Barth, R.F, Vicente, M.G, Harling, O.K., Kiger, W.S., Riley, K.J., Binns, P.J., Wagner, F.M, Suzuki, M., Aihara, T., Kato, I., Kawabata, S., 2012. Current status of boron neutron capture therapy of high grade gliomas and recurrent head and neck cancer. Radiat. Oncol. 7:146.

Bielack, S., Carrle, D., Casali, P.G., 2009 ESMO guidelines working group. Osteosarcoma: ESMO clinical recommendations for diagnosis, treatment and follow-up. Ann. Oncol. 20(Suppl. 4):137–9.

Bortolussi, S. and Altieri, S., 2013. Boron Concentration Measurement in Biological Tissues by Charged Particles Spectrometry. Rad. Env. Biophys. 52:493–503.

Bortolussi, S., Postuma, I., Protti, N., Provenzano, L., Ferrari, C., Cansolino, L., Dionigi, P., Galasso, O., Gasparini, G., Altieri, S., Miyatake, S.I., González, S.J., 2017. Understanding the potentiality of Accelerator Based-Boron Neutron Capture Therapy for osteosarcoma: dosimetry assessment based on the reported clinical experience. Rad. Onc. 12(1), 130.

Durrani, S.A., Bull, R.K., 1987. Solid state nuclear track detection: principles, methods and applications. International Series in Natural Philosophy (Ed. D. terHaar), Pergamon Press, Oxford.

Fleischer, R. L., Price, P. B., Walker, R. M., 1975. Nuclear Tracks in Solids. University of California Press, Berkeley.

Farías, R., Garabalino, M., Ferraris, S., Santa María, J., Rovati, O., Lange, F., Trivillin, V.A., Monti Hughes, A., Pozzi, E.C.C, Thorp, S.I., Curotto, P., Miller, M., Santa Cruz, G.A.,

Bortolussi, S., Altieri, S., Portu, A.M., Saint Martin, G., Schwint, A.E., Gonzalez, S.J., 2015. Toward a clinical application of ex situ boron neutron capture therapy for lung tumors at the RA-3 reactor in Argentina. Med. Phys. 42:4161-4173.

Ferrari, C., Zonta, C., Cansolino, L., Clerici, A.M., Gaspari, A., Altieri, S., Bortolussi, S., Stella, S., Bruschi, P., Dionigi, P., Zonta, A., 2009. Selective uptake of p-boronophenylalanine by osteosarcoma cells for boron neutron capture therapy. Appl. Radiat. Isot. 67:S341-4.

Futamura, G., Kawabata, S., Siba, H., Kuroiwa, T., Suzuki, M., Kondo, N., Ono, K., Sakurai, Y., Tanaka, M., Todo, T., Miyatake, S.I., 2014. A case of radiation-induced osteosarcoma treated effectively by boron neutron capture therapy. Radiat. Oncol. 9: 237.

González, S.J., Bonomi, M.R., Santa Cruz, G.A., Blaumann, H.R., Calzetta Larrieu, O.A., Menéndez, P., Jiménez Rebagliati, R., Longhino, J., Feld, D.B., Dagrosa, M.A., Argerich, C., Castiglia, S.G., Batistoni, D.A., Liberman, S.J., Roth, B.M., 2004. First BNCT treatment of a skin melanoma in Argentina: dosimetric analysis and clinical outcome. Appl. Radiat. Isot. 61(5):1101-1105.

Image-Pro Plus Reference Guide, Media Cyberneics Inc., United States 2009.

ICRU Report No. 46. 1992. Photon, electron, proton and neutron interaction data for body tissues.

Johnson, T.B., Axelsson, R., and Johansson, S.A.E., 1970. X-ray analysis: Elemental trace analysis at the 10 -12 g level Nucl. Instr. Meth. 84, 141

Jolivet, M., Lebatard, E., Reyss, J.L., Bourlès, D., Mackaye, H.T., Lihoreau, F., Vignaud, P., Brunet M., 2008. Can fossil bones and teeth be dated using fission track analysis?. Chem. Geol. 247:81–99.

Kankaanranta, L., Seppälä, T., Koivunoro, H., Saarilahti, K., Atula, T., Collan, J., Salli, E., Kortesniemi, M. et al., 2012. Boron neutron capture therapy in the treatment of locally recurred head-and-neck cancer: Final analysis of a Phase I/II trial". Int. J. Rad. Onc. Bio. Phys. 82.

Kato, I., Ono, K., Sakurai, Y., Ohmae, M., Maruhashi, A., Imahori, Y., Kirihata, M., Nakazawa, M., Yura, Y., 2004. Effectiveness of BNCT for recurrent head and neck malignancies. Appl. Radiat. Isot. 61(5):1069-73.

Locher, G.L., 1936. Biological effects and therapeutic possibilities of neutrons. Am. J. Roengenol. Radium. Ther. 36(1):1-11.

Maxwell, J.A., Campbell, J.L. and Teesdale, W.J., 1989. Nucl. Instr. and Meth. B 43 ,218.

Nikezic, D., Yu, K.N., 2004. Formation and growth of tracks in nuclear track materials. Mater. Sci. Eng. R 46:51–123.

Portu, A., Bernaola, O.A., Nievas, S., Liberman, S., Saint Martin, G., 2011. Measurement of 10B concentration through autoradiography images in polycarbonate nuclear track detectors. Rad. Meas. 46:1154-1159.

Portu, A., Molinari, A.J., Thorp, S.I., Pozzi, E.C., Curotto, P., Schwint, A.E, Saint Martin, G., 2015a. Neutron autoradiography to study boron compound microdistribution in an oral cancer model. Int. J. Radiat. Biol. 91(4):329-35.

Portu, A., Postuma, I., Gadan, M.A., Saint Martin, G., Olivera, M.S., Altieri, S., Protti, N., Bortolussi, S., 2015b. Inter-comparison of boron concentration measurements at INFN-University of Pavia (Italy) and CNEA (Argentina). Appl. Radiat. Isot. 105:35–39.

Postuma, I., Ristori, S., Panza, L., Ballarini, F., Bortolussi, S., Protti, N., Altieri, S., Ferrari, C., Cansolino, L., Bruschi, P., 2016. An improved neutron autoradiography set-up for 10B concentration measurements in biological samples. Rep. Pract. Oncol. Radiother. 21(2):123-128.

Provenzano, L., González, S.J., Altieri, S., Bruschi, P., Olivera, M.S., Portu, A.M., Postuma, I., Bortolussi, S., 2014. Extension of the alpha spectrometry technique for boron measurements in bone. 16th International Congress on Neutron Capture Therapy. Helsinki, Finland.

Provenzano, L., Rodríguez, L.M., Fregenal, D., Bernardi, G., Olivares, C., Altieri, S., Bortolussi, S. and González, S.J., 2015. Measuring the stopping power of αparticles in compact bone for BNCT. J. Phys.: Conf. Ser. 583-012047.

Saint Martin, G., Portu, A., Santa Cruz, G.A., Bernaola, O.A., 2011. Stochastic simulation of track density in nuclear track detectors for 10B measurements in autoradiography. Nucl. Instr. Meth. Phys. B 269:2781-2785.

Skoog, D.A. and Leary, J.J., 1996. Principles of instrumental Analysis. 4th ed. Mc. Graw Hill.

Suzuki, M., Sakurai, Y., Masunaga, S., Kinashi, Y., Nagata, K., Maruhashi, A., et al., 2006. Feasibility of boron neutron capture therapy (BNCT) for malignant pleural mesothelioma from a viewpoint of dose distribution analysis. Int. J. Radiat. Oncol. Biol. Phys. 66:1584-1589.

Wang, L.W., Wang, S.J., Chu, P.Y., Ho, C.Y., Jiang, S.H, Liu, Y.W.H., Liu, Y.H, Liu, H.M et al. 2011 BNCT for locally recurrent head and neck cancer: Preliminary clinical experience from a phase I/II trial at TsingHua Open-Pool Reactor". Appl. Radiat. Isot. 69 (12): 1803–6.

Yanagie, H., Higashi, S., Seguchi, K., Ikushima, I., Fujihara, M., Nonaka, Y., Oyama, K., Maruyama, S., Hatae, R., Suzuki, M., Masunaga, S., Kinashi, T., Sakurai, Y., Tanaka, H., Kondo, N., Narabayashi, M., Kajiyama, T., Maruhashi, A., Ono, K., Nakajima, J., Ono, M., Takahashi, H., Eriguchi, M., 2014. Pilot clinical study of boron neutron capture therapy for

recurrent hepatic cancer involving the intra-arterial injection of a (10)BSH-containing WOW emulsion. Appl. Radiat. Isot. 88:32-7.

Ziegler, J.F., Littmark, U. and Biersack, J.P., 1985. The stopping and range of ions in solids. Pergamon New York.

Zonta, A., Prati, U., Roveda, L., Ferrari, C., Zonta, S., Clerici, A.M., Zonta, C., Pinelli, T., Fossati, F., Altieri, S., Bortolussi, S., Bruschi, P., Nano, R., Barni, S., Chiari, P., Mazzini, G., 2006. Clinical lessons from the first applications of BNCT on unresectable liver metastases. J. Phys.: Conf. Ser. 41:484-495.